

Comparative Study on Interfacial Traps in Organic Thin-Film Transistors According to Deposition Methods of Organic Semiconductors

Jae-Hoon Park* · Jin-Hyuk Bae**†

*Department of Electronic Engineering, Hallym University, Chuncheon 200-702, Korea

**School of Electronics Engineering, Kyungpook National University, Daegu 702-701, Korea

(Received May 21, 2013 ; Revised June 26, 2013 ; Accepted June 26, 2013)

Abstract : We analysed interfacial traps in organic thin-film transistors (TFTs) in which pentacene and 6,13-bis(triisopropylsilylethynyl)-pentacene (TIPS-pentacene) organic semiconductors were deposited by means of vacuum-thermal evaporation and drop-coating methods, respectively. The thermally-deposited pentacene film consists of dendritic grains with the average grain size of around 1 μm , while plate-like crystals over a few hundred microns are observed in the solution-processed TIPS-pentacene film. From the transfer characteristics of both TFTs, lower subthreshold slope of 1.02 V/decade was obtained in the TIPS-pentacene TFT, compared to that (2.63 V/decade) of the pentacene transistor. The interfacial trap density values calculated from the subthreshold slope are about $3.4 \times 10^{12}/\text{cm}^2$ and $9.4 \times 10^{12}/\text{cm}^2$ for the TIPS-pentacene and pentacene TFTs, respectively. Herein, lower subthreshold slope and less interfacial traps in TIPS-pentacene TFTs are attributed to less domain boundaries in the solution-processed TIPS-pentacene film.

Keywords : transistor, organic semiconductor, interface trap, vacuum deposition, solution process.

1. INTRODUCTION

Organic thin-film transistors (TFTs) have great potential for use in various electronic applications such as flat-panel displays, radio-frequency identification tags, and smart cards due to their advantages such as low-temperature and large-area processability [1-6]. For the fabrication of these TFTs, deposited by means of vacuum (e.g. molecular beam epitaxy and thermal evaporation, etc.) or

organic semiconductors (OSCs) are generally solution (e.g. drop-coating and various printing technologies) processes. Besides, there are two different types of gate insulator (GI) materials used for organic TFTs, one of which is categorized into an inorganic GI and the other into an organic one. In the literature, it is well recognized that polymer-based organic GIs, such as poly(4-vinylphenol), polystyrene, and polyvinyl cinnamate, are much favorable to organic TFTs because they can be deposited

†Corresponding author (E-mail : jhbae@ee.knu.ac.kr)

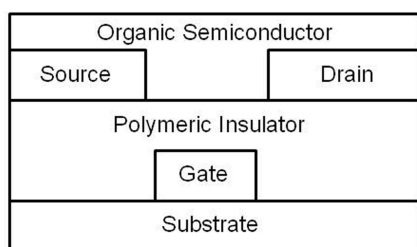
by simple coating of polymer solutions and their mechanical flexibility is much beneficial for the application of organic transistors to flexible electronics [7–10]. Note that inorganic GIs, such as silicon dioxide and silicon nitride, usually require high-processing temperatures above 150 °C and they are brittle as well, which inevitably limit the process compatibility with plastic substrates. Therefore, polymeric GIs are widely used for organic TFTs to date. However, in contrast to the GI case, various methods for OSC deposition are still competing, which reflects the significance of patterned and crystalline growth of OSCs on aspects of the TFT performance. In detail, vacuum deposition of OSCs is capable of ordered growth of organic molecules by controlling the deposition rate and substrate temperature as well as patterned growth with micron resolution by using a shadow mask. On the other hand, solution-based processes are advantageous for simple deposition of OSCs on specific locations under atmospheric pressure, thereby allowing the fabrication of large arrays of organic TFTs and complex circuits over large areas. From the technical point of view, previous studies may provide ample approaches for low-cost manufacturing of organic electronics devices. Nevertheless, a rather comprehensive study is still required to understand the electrical characteristics of organic TFTs influenced by the deposition method of OSCs.

In this work, we have fabricated organic TFTs in which pentacene and 6,13-bis(triisopropylsilylethynyl)-pentacene (TIPS-pentacene) organic semiconductors were deposited by means of vacuum-thermal evaporation and drop-coating methods, respectively. The surface morphologies of vacuum-deposited pentacene and solution-processed TIPS-pentacene films and the corresponding TFT properties are presented together with the analysis results of interfacial traps in the TFTs.

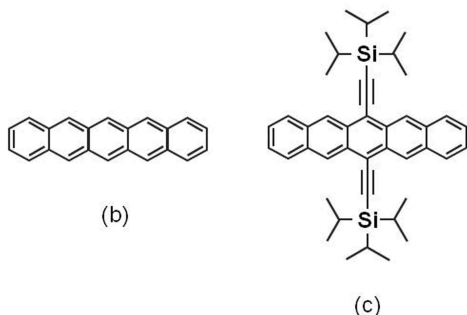
2. EXPERIMENTAL PROCEDURE

2.1. Fabrication of organic TFTs

A bottom-gate/bottom-contact TFTs shown in Fig. 1(a) was fabricated on glass substrates with prepatterned indium-tin-oxide (ITO) gate electrodes (sheet resistance: $\sim 20 \Omega$ per square). The ITO-patterned glass substrates were cleaned up with acetone, isopropyl alcohol, methanol, and deionized water in sequence. As a GI for our TFTs, poly(4-vinylphenol) (PVP) (Sigma Aldrich, approximately 3 wt.% dissolved in propylene glycol methyl ether acetate) was mixed with a cross-linking agent, methylated poly(melamine-co-formaldehyde) [11]. The PVP solution was spin-coated on top of the ITO-patterned glass substrate and baked at 200 °C for 1 hr, followed by pre-curing at 100 °C for 1 min. The thickness and the capacitance per unit area (C_i) of the cross-linked PVP GI film were about 100 nm and 34 nF/cm². Then, 60-nm-thick source and drain electrodes were formed by thermally depositing Au through a shadow mask onto the GI-coated substrates at a rate of 0.01 nm/s under a base pressure of $\sim 1 \times 10^{-5}$ Torr. Finally, two different OSCs were deposited onto the substrates to complete the fabrication of organic TFTs. In detail, pentacene (Sigma Aldrich, used without further purification) were thermally deposited at a rate of 0.05 nm/s under a base pressure of $\sim 1 \times 10^{-6}$ Torr. Meanwhile, TIPS-pentacene (Sigma Aldrich, 1 wt.% dissolved in Anisole) was drop-casted onto the substrate and thermally cured at 60 °C for 3 min [12]. Fig. 1(b) and 1(c) depict the chemical structures of pentacene and TIPS-pentacene molecules; the main-backbone structure consisting of five linearly-fused benzene rings is exactly the same for both materials. The channel length (L) and width (W) of our organic TFTs were 50 and 1000 μ m, respectively.



(a)



(b)

(c)

Fig. 1. (a) Schematic representation of the fabricated organic TFTs with a polymeric GI. Chemical structures of (b) pentacene and (c) TIPS-pentacene.

2.2. Characterizations of OSC films and organic TFTs

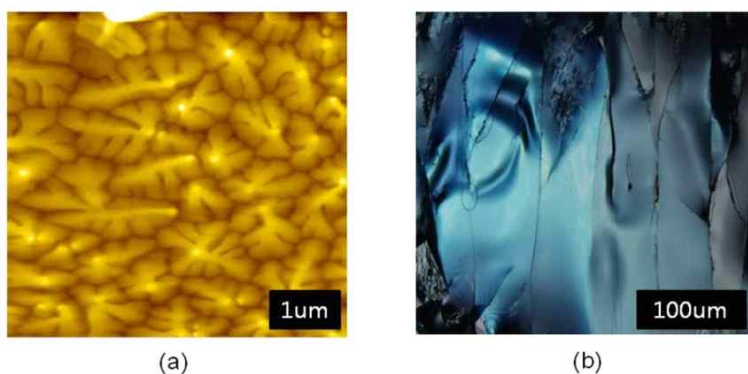
The surface morphologies of vacuum-deposited pentacene and solution-processed TIPS-pentacene films were observed with an

atomic force microscope (AFM) (XE150, PSIA Inc.) and optical microscope, respectively. The electrical characterization of the fabricated organic TFTs were undertaken, in the dark and in ambient air, using a semiconductor parameter analyzer (EL 421C, Elecs Co.).

3. RESULTS AND DISCUSSION

3.1. Morphological images of OSC films

Figure 2(a) shows the AFM image of the vacuum-deposited pentacene film which was grown on the cross-linked PVP layer. Typical surface morphology of pentacene films consisting of dendritic grains is clearly observed [13,14]; the average grain size was approximately 1 μm in our result. On the other hand, the TIPS-pentacene film drop-casted onto the cross-linked PVP layer shows elongated plate-like crystals over a few hundreds microns as shown in Fig. 2(b). It should be pointed out that TIPS-pentacene crystals are definitely larger in size than pentacene grains. In general, the film formation of thermally-evaporated pentacene molecules is known to proceed through the transition from generation of multiple nuclei then to two and three dimensional growth [15,16]. Contrastively, TIPS-pentacene molecules in



(a)

(b)

Fig. 2. (a) Atomic force microscopic image of the vacuum-deposited pentacene film. (b) Optical microscopic image of the solution-processed TIPS-pentacene film.

dilute solution are initially condensed together to form nucleation points and continue to grow into larger crystals during the evaporation of a chemical solvent. As the generation of nucleation points is intimately influenced by the evaporation rate of the solvent, it was also reported that slower evaporation rate contributes to larger crystalline growth of TIPS-pentacene molecules up to a few millimeters in length [6]. The clear distinction in the surface morphology between vacuum-deposited pentacene and solution-processed TIPS-pentacene films in our study can be thus attributed to the different growth kinetics of OSC molecules depending on the deposition method. Accordingly, it is evident that the solution-processed TIPS-pentacene film will have less domain boundaries in the conducting channel of TFTs.

3.2. Electrical characteristics of organic TFTs

Figure 3 shows the output characteristic curves of the fabricated organic TFTs. The drain currents (I_D) as a function of the drain voltage (V_D) were obtained with varying the gate voltage (V_G) from -2 V to -5 V in -1 V increments. Here, we would like to note that the operating voltage for both TFTs is below

-5 V, demonstrating the low-voltage operation of our TFTs; organic TFTs typically operate at above -30 V [16,17]. It is likely due to the thin thickness of cross-linked PVP GI without any structural defects. Figure 4(a) and 4(b) show the corresponding transfer characteristic curves of the pentacene and TIPS-pentacene TFTs in this study. The field-effect mobility (μ_{sat}) in the saturation region was calculated by the following equation of

$$\mu_{sat} = \frac{2L}{W \times C_i} \times \frac{I_D}{(V_G - V_T)^2},$$

where V_T is the threshold voltage [18]. The extracted μ_{sat} values are 0.62 cm^2/Vs for the vacuum-deposited pentacene TFT and 0.20 cm^2/Vs for the solution-processed TIPS-pentacene TFT, respectively. The fact that the charge transport in an OSC film and field-effect mobility of an organic TFT are strongly governed by the OSC material itself indicates that the higher μ_{sat} value for the pentacene transistor TFT can be a result of an efficient π -orbital overlap in the pentacene film. However, it is not plausible to judge the charge trapping behavior from the obtained μ_{sat} values in both TFTs because a trap-filling mostly occurs in the saturation region (i.e. $V_G > V_T$). On this account, interfacial traps in

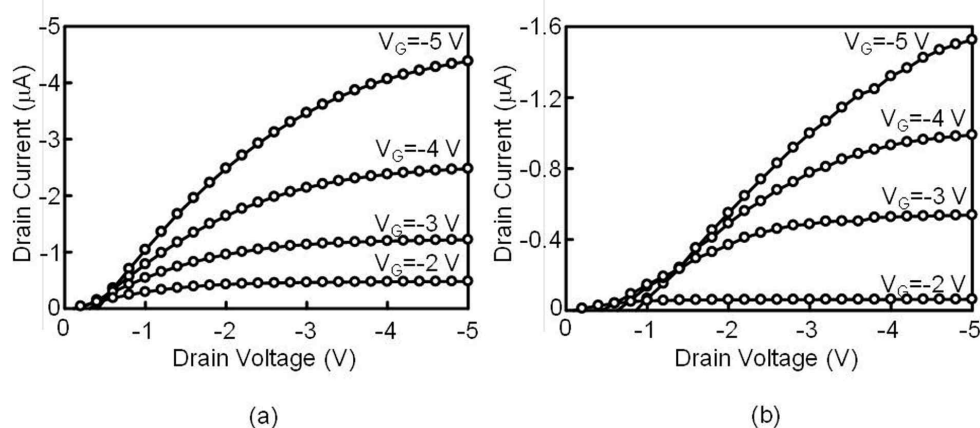


Fig. 3. Output characteristic curves of the fabricated TFT having (a) the vacuum-deposited pentacene and (b) solution-processed TIPS-pentacene films.

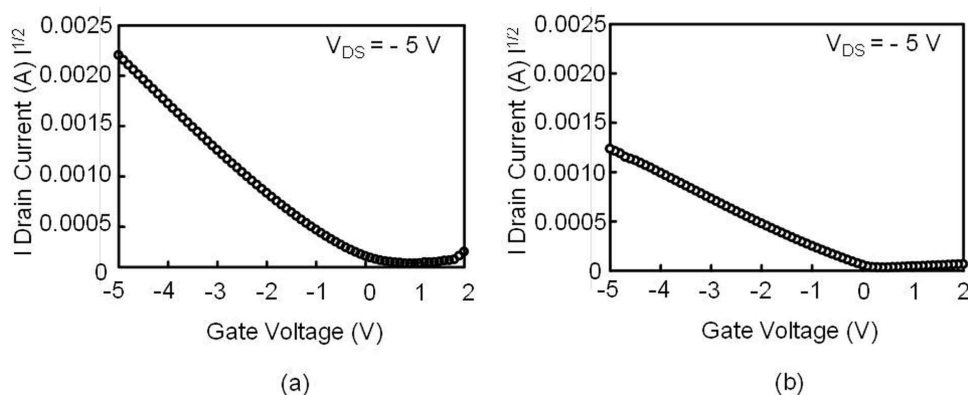


Fig. 4. Transfer characteristic curves of the fabricated TFT having (a) the vacuum-deposited pentacene and (b) solution-processed TIPS-pentacene films. The applied V_D was -5 V.

organic TFTs should be evaluated in the subthreshold region [19].

3.3. Analysis of interfacial traps in organic TFTs

Let us now examine how interfacial traps are affected by the deposition method of an OSC film on a solution-processed GI layer. Note that the interfacial trap density (N_{it}) is directly related to the subthreshold slope (SS) which is an important parameter in relation to a switching speed from an off-state to an on-state in the TFT. The SS can be obtained using the following equation [20],

$$SS = \frac{\partial V_G}{\partial(\log I_D)}.$$

Interestingly, the SS (2.63 V/decade) for the vacuum-deposited pentacene TFT is quite higher than that (1.02 V/decade) for the solution-processed TIPS-pentacene device. From the obtained SS values, the N_{it} can be calculated by the equation of

$$N_{it} \approx \left[\frac{q}{kT} \times SS \times \log e - 1 \right] \times \frac{C_i}{q},$$

where q is the electronic charge, k is the Boltzmann's constant, T is the temperature, and e is the base of the natural logarithm

[21]. The obtained N_{it} was $9.4 \times 10^{12}/\text{cm}^2$ for the vacuum-processed pentacene OTFT and $3.4 \times 10^{12}/\text{cm}^2$ for the solution-processed TIPS-pentacene OTFT. It is found that the solution-processed TIPS-pentacene TFT exhibits less N_{it} compared to the vacuum-deposited pentacene case, implying the significant role of grain/domain boundaries on the charge trapping behavior in the TFT in line with the previous works [15,19]. Note that the drop-casted TIPS-pentacene film showed larger plate-like crystals with their size over a few hundred microns in Fig. 2(b) and thus less boundaries exist in the conducting channel of the transistor. The results suggest that solution processes for the OSC deposition are more advantageous for enlarging OSC crystals and reducing interfacial traps in organic TFTs, which is expected to enhancing the switching speed of organic TFTs in various integrated logic circuits.

4. CONCLUSION

We have investigated how interfacial traps in organic TFTs are affected by the deposition method of an OSC film. In comparison with the vacuum-deposited pentacene case, the

solution-processed TIPS-pentacene film exhibit larger elongated plate-like crystals, which could be explained in terms of the different growth kinetics of OSCs according to the deposition method. Consequently, less domain boundaries could be produced in the TIPS-pentacene film, resulting in less interfacial trap density, N_{it} , in the TFT. These results are of prime importance to develop low-cost and high-speed organic electronics. In order to enhance the field-effect mobility of solution-processed organic TFTs, further studies on the orientational control of OSC molecules should be progressed.

Acknowledgments

This research was supported by Hallym University Research Fund, 2013 (HRF-201303-005) and Basic Science Research Program through the National Research Foundation of Korea(NRF) funded by the Ministry of Education(2013009807).

References

1. G. H. Gelinck, H. E. Huitema, E. V. Veenendall, E. Cantatore, L. Schrijnemakers, J. B. P. H. V. D. Putten, T. C. T. Genus, M. Beenhakkers, J. B. Giesbers, B.-H. Huisman, E. J. Meijer, E. M. Benito, F. J. Touwslager, A. W. Marsman, B. J. E. V. Rens, D. M. De. Leeuw, "Flexible Active-Matrix Displays and Shift Registers Based on Solution-Processed Organic Transistors", *Nat. Mater.* **3**, 106 (2004).
2. Z.-T. Zhu, J. T. Mason, R. Dieckmann, G. G. Malliaras, "Humidity Sensors Based on Pentacene Thin-Film Transistors", *Appl. Phys. Lett.* **81**, 4643 (2002).
3. D. Voss, "Cheap and Cheerful Circuits", *Nature* **407**, 442 (2000).
4. T. Sekitani, H. Nakajima, H. Maeda, T. Fukushima, T. Aida, K. Hata, T. Someya, "Stretchable Active-Matrix Organic Light-Emitting Diode Display Using Printable Elastic Conductors", *Nat. Mater.* **8**, 494 (2009).
5. H. Sirringhaus, T. Kawase, R. H. Friend, T. Shimoda, M. Inbasekaran, W. Wu, E. P. Woo, "High-Resolution Inkjet Printing of All-Polymer Transistor Circuits", *Science* **290**, 2123 (2000).
6. H. B. Akkerman, H. Li, Z. Bao, "TIPS-Pentacene Crystalline Thin Film Growth", *Org. Electron.* **13**, 2056 (2012).
7. H. Sirringhaus, R. J. Wilson, R. H. Friend, "Mobility Enhancement in Conjugated Polymer Field-Effect Transistors Through Chain Alignment in a Liquid-Crystalline Phase", *Appl. Phys. Lett.* **77**, 406 (2000).
8. W.-Y. Chou, H.-L. Cheng, "High Mobility Pentacene Thin-Film Transistors on Photopolymer Modified Dielectrics", *Adv. Funct. Mater.* **14**, 811 (2004).
9. J.-H. Bae, J. Kim, W.-H. Kim, S.-D. Lee, "Importance of the Functional Group Density of a Polymeric Gate Insulator for Organic Thin-Film Transistors", *Jpn. J. Appl. Phys.* **46**, 385 (2007).
10. M.-H. Kim, S.-P. Noh, C.-M. Keum, J.-H. Bae, S.-D. Lee, "Bias Voltage Effect on Electrical Properties of N-Type Polymeric Field Effect Transistors with Dual Gate Electrodes", *Org. Electron.* **13**, 2365 (2012).
11. S. C. Lim, S. H. Kim, J. B. Koo, J. H. Lee, C. H. Ku, Y. S. Yang, Y. Zyung, "Hysteresis of Pentacene Thin-Film Transistors and Inverters with Cross-Linked Poly(4-vinylphenol) Gate Dielectrics", *Appl. Phys. Lett.* **90**, 173512 (2007).
12. C.-M. Keum, J.-H. Bae, W.-H. Kim, M.-H. Kim, J. Park, S.-D. Lee, "Effect of Thermo-Gradient-Assisted Solvent Evaporation on the Enhancement of the Electrical Properties of 6,13-Bis(triisopropylsilyl ethynyl)-Pentacene

- Thin-Film Transistors”, *J. Korean Phys. Soc.* **58**, 1479 (2011).
13. A.-L. Deman, M. Erouel, D. Lallemand, M. Phaner-Goutorbe, P. Lang, J. Tardy, “Growth Related Properties of Pentacene Thin Film Transistors with Different Gate Dielectrics”, *J. Non-Cryst. Solids* **354**, 1598 (2008).
 14. J.-H. Bae, W.-H. Kim, C.-J. Yu, and S.-D. Lee, “Reduction in Contact Resistance of Pentacene Thin-Film Transistors by Formation of an Organo-Metal Hybrid Interlayer”, *Jpn. J. Appl. Phys.* **48**, 020209 (2009).
 15. J. Park, J.-H. Bae, W.-H. Kim, S.-D. Lee, J. S. Gwag, D. W. Kim, J. C. Noh, J. S. Choi, “The Surface Energy-Dictated Initial Growth of a Pentacene Film on a Polymeric Adhesion Layer for Field-Effect Transistors”, *Solid-State Electron.* **54**, 1650 (2010).
 16. S. Y. Cho, J. M. Ko, J. Y. Jung, J. Y. Lee, D. H. Choi, C. Lee, “Ink-Jet Printed Organic Thin Film Transistors Based on TIPS Pentacene with Insulating Polymers”, *J. Mater. Chem. C* **1**, 914 (2013).
 17. M. W. Lee, G. S. Ryu, Y. U. Lee, C. Pearson, M. C. Petty, C. K. Song, “Control of Droplet Morphology for Ink-Jet-Printed TIPS-Pentacene Transistors”, *Microelectron. Eng.* **95**, 1 (2012).
 18. C. D. Dimitrakopoulos, D. J. Maseo, “Organic Thin-Film Transistors: A Review of Recent Advances”, *IBM J. Res. Dev.* **45**, 11 (2001).
 19. J. Park, Y.-S. Jeong, K.-S. Park, L.-M. Do, J.-H. Bae, J. S. Choi, C. Pearson, M. Petty, “Subthreshold Characteristics of Pentacene Field-Effect Transistors Influenced by Grain Boundaries”, *J. Appl. Phys.* **111**, 104512 (2012).
 20. J. B. Choi, D. C. Yun, Y. I. Park, J. H. Kim, “Properties of Hydrogenated Amorphous Silicon Thin Film Transistors Fabricated at 150°C”, *J. Non-Cryst. Solids* **266**, 1315 (2000).
 21. A. Rolland, J. Richard, J. P. Kleider, D. Mencaraglia, “Electrical Properties of Amorphous Silicon Transistors and MIS-Devices: Comparative Study of Top Nitride and Bottom Nitride Configurations”, *J. Electrochem. Soc.* **140**, 3679 (1993).